

On the NMR Satellites in the $X_2(Y_{1-v}Z_v)$ Type Heusler Alloys

著者	Nakamichi Takuro
journal or publication title	Science reports of the Research Institutes, Tohoku University. Ser. A, Physics, chemistry and metallurgy
volume	30
page range	60-85
year	1981
URL	http://hdl.handle.net/10097/28203

On the NMR Satellites in the $X_2(Y_{1-\nu}\eta_\nu)Z$ Type
Heusler Alloys *

Takurô Nakamichi

The Research Institute for Iron, Steel and Other Metals

(Received June 9, 1981)

Synopsis

In the development of Niculescu et al.'s idea, the general expression of the hyperfine field of the nucleus in the Heusler alloy, $X_2(Y_{1-\nu}\eta_\nu)Z$ containing the impurity η is derived on the basis of the phenomenological relation between the moment and the local environment variable indicating the impurity arrangement around the nucleus. The expression is applied to several NMR experimental results and gives a satisfactory interpretation of the NMR satellites as well as the phenomenological coefficients in $Fe_{3-x}V_xSi$ and $Fe_{3-x}Mn_xSi$ alloy systems. The coefficients are in good agreement with those obtained independently in Fe_3Z and Co_2MnZ alloy systems. The analysis of the NMR spectrum of $Mn_2V_{1-y}Al_{1+y}$ alloy suggests that V atom should have the magnetic moment in addition to Mn in this alloy.

I. Introduction

Heusler alloy is formed in a ternary alloy system X-Y-Z with X_2YZ composition, having the double ordered structure¹⁾ $L2_1$ as illustrated in Fig. 1. For a long time it has been studied only in the type of X_2MnZ constitution since the discovery of the ferromagnetic Cu_2MnAl by Heusler²⁾ but recently many Heusler alloys have been found as indicated in Table 1.

If one tries to arrange the constituent elements in these alloys in the order of Y, X and Z, it may be found that the arrangement is in accordance with the element order in the periodic table as confirmed in Table 1. Therefore, most of X and Y atoms belong to the transition metal series and thus show frequently magnetic activity in the alloy. The transition metal capable to be magnetic occupies either A,

* The 1742th report of the Research Institute for Iron, Steel and Other Metals

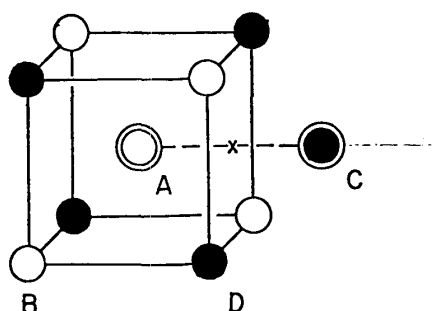


Fig. 1. The crystal structure of the Heusler alloy X_2YZ . X occupies A and C sites. While Y and Z occupy B and D site respectively.

Table 1. List of the Heusler alloy and its magnetism (magnetic transition temperature [K]). F: ferromagnetism, A: antiferromagnetism, CP: constant paramagnetism, TP: temperature dependent paramagnetism, CS: canted spin structure, SS: spiral spin structure, HA: helical spin structure. * Tetragonal deformed.

YX_2Z (Ref.)	Remark	YX_2Z (Ref.)	Remark	YX_2Z (Ref.)	Remark	YX_2Z (Ref.)	Remark
LiMg ₂ Tl(3)		HfCo ₂ Al(4)	F(193)	CrFe ₂ Si(6)		MnPt ₂ Al(4)	A(190)
KNa ₂ Sb(3)		HfCo ₂ Ga(4)	F(186)	CrCo ₂ Ga(3)		MnPt ₂ Ga(4)	A(75)
CsK ₂ Sb(3)		HfCo ₂ Sn(4)	F(394)	CrRh ₂ Sn(7)*		MnCu ₂ Al(4)	F(630)
		HfNi ₂ Al(3)				MnCu ₂ Ga(3)	
MgNi ₂ In(3)		HfNi ₂ Ga(3)		Mn ₃ Si(8)	HA(26)	MnCu ₂ In(4)	F(500)
MgNi ₂ Sn(3)		HfNi ₂ Sn(4)	CP	MnFe ₂ Al(3)		MnCu ₂ Sn(4)	F(530)
MgNi ₂ Sb(3)		HfCu ₂ Al(3)		MnFe ₂ Si(4)	CS(210)	MnCu ₂ Sb(3)	
MgAg ₂ Zn(3)				MnCo ₂ Al(4)	F(693)	MnAg ₂ Al(3)	
		VmN ₂ Al(4)	F(678)	MnCo ₂ Ga(4)	F(694)	MnAg ₂ Au(3)	
TiFe ₂ Ga(3)		VFe ₂ Ga(5)	TP	MnCo ₂ Si(4)	F(985)	MnAu ₂ Al(4)	SS(200)
TiFe ₂ Sn(4)	TP	VFe ₂ Si(6)	TP	MnCo ₂ Ge(4)	F(905)	MnAu ₂ In(9)	Mag. ord.
TiCo ₂ Al(4)	F(138)	VCo ₂ Al(4)	F(310)	MnCo ₂ Sn(4)	F(829)		
TiCo ₂ Ga(4)	F(130)	VCo ₂ Ga(4)	F(349)	MnCo ₂ Sb(4)	F	Fe ₃ Al(10)	F(750)
TiCo ₂ Si(3)		VCo ₂ Si(3)		MnRh ₂ Al(4)	F(26)	Fe ₃ Ga(10)	F(730)
TiCo ₂ Ge(3)		VCo ₂ Sn(4)	F(70)	MnRh ₂ Ge(4)	F(450)	Fe ₃ Si(10)	F(805)
TiCo ₂ Sn(4)	F(359)	VRh ₂ Sn(7)		MnRh ₂ Sn(4)	F(412)	FeCo ₂ Ga(11)	F(1060)
TiCo ₂ Sb(3)		VNi ₂ Ga(3)		MnIr ₂ Ga(4)	A	FeCo ₂ Si6	F
TiNi ₂ Al(3)		VNi ₂ Sn(4)	CP	MnNi ₂ Al(4)	HA(300)	FeRh ₂ Sn(4)*	F(583)
TiNi ₂ Ga(3)				MnNi ₂ Ga(4)	F(379)	FeCu ₂ Sn(3)	
TiNi ₂ In(3)		NbCo ₂ Al(3)		MnNi ₂ In(4)	F(323)		
TiNi ₂ Sn(4)	CP	NbCo ₂ Ga(3)		MnNi ₂ Ge(3)		CoRh ₂ Sn(4)*	F(444)
TiCu ₂ In(3)		NbCo ₂ Sn(4)*	F(119)	MnNi ₂ Sn(4)	F(410)	CoCu ₂ Sn(3)	
		NbNi ₂ Al(3)		MnNi ₂ Sb(4)	F(360)		
ZrCo ₂ Al(4)	F(185)	NbNi ₂ Ga(3)		MnPd ₂ Al(4)	A(240)	NiRh ₂ Sn(7)	
ZrCo ₂ Sn(4)	F(444)	NbNi ₂ Sn(4)	CP	MnPd ₂ In(4)	A(142)	NiCu ₂ Sn(3)	
ZrNi ₂ Al(3)				MnPd ₂ Ge(4)	F(260)		
ZrNi ₂ Sn(4)	CP	TaCo ₂ Al(3)		MnPd ₂ Sn(4)	F(189)	CuRh ₂ Sn(7)	
ZrCu ₂ Al(3)		TaCo ₂ Ga(3)		MnPd ₂ Sb(4)	F(247)	CuZn ₂ Au(3)	
		TaNi ₂ Al(3)					
						AgCd ₂ Au(3)	
						AgZn ₂ Au(3)	

C atomic sites as X or B site as Y with and without other magnetic element in other atomic site. Such a various scheme of the arrangement

of the magnetic atom makes the Heusler alloy suitable to the study of the local environment effect upon the magnetic or electronic state of the transition metal.

To observe the environment effect on the magnetic state of the transition metal, it is usual to vary the combination of the constitution of the alloy keeping one or two elements unchanged. Another technique is, however, also developed by substituting X, Y or Z atom by ξ , η or ζ impurity in a X_2YZ alloy and produces an interesting systematic variation of magnetic properties with alloy composition. Especially, in the NMR spectrum such a procedure produces a characteristic satellite structure, which cannot be observed in the stoichiometric composition. It is the reason to study the NMR satellite structure in detail in the present work.

As shown in Fig. 2, the main and satellite peaks indicated as the same group are all produced by the nuclei of the same kind of atoms in the same crystallographic atomic sites. Therefore, the difference between them should be ascribed to the difference of the local environment, in which they are situated.¹²⁾

Niculescu et al.⁶⁾ have found the resonance peak position of the main and satellite peaks do not so vary with alloy composition and only the relative intensity of each resonance peak varies so remarkably in $Fe_{3-x}V_xSi$ and $Fe_{3-x}Mn_xSi$ alloys. They proposed that each resonance peak position is specified by the number of the excess V or Mn atom in the B site in the near neighbour atomic shell around the nucleus concerned through the variation of the atomic moment of each Fe atom in the A,C sites influenced by the excess atoms in its 1st neighbour. Combining the conventional hyperfine field expression with the variation of the atomic moment of Fe atoms in the A,C sites, they could explain the essential features of the NMR satellite structure of these two alloys.

However, they did not formalize their idea to establish the relation between the hyperfine field and the observed moment and therefore did not mention several important features of the NMR spectrum obtained experimentally and furthermore did not try to analyse the intensity of the spectrum. Therefore, in the present paper as a

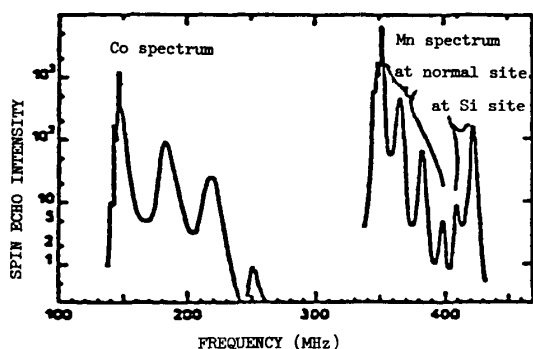


Fig. 2. NMR spin echo spectrum of $Co_2Mn_{1.04}Si_{0.96}$ at 4.2 K by Grover et al. (ref. to 12)).

development of their idea, the specification of the atom due to the local environment is more satisfactorily defined by introducing the environment variable \hat{q}_W (II), and the moment variation with the environment variable is defined and calculated including the induced moment effect according to a certain fundamental formula proposed at present (III) and the hyperfine field expression of each constituent atom qualified by the environment variable is derived from the fundamental formula (IV). Furthermore, several equations to determine the important phenomenological coefficients, which is convenient to the experimental analysis, are given and their usefulness and justification are examined by comparison with various experiments including the analysis of the intensity of the NMR spectra (V,VI).

II. Classification of Atom by Environment Variable

In a Heusler alloy X_2YZ with $L2_1$ structure as shown in Fig. 1, X atom occupies the A,C atomic sites and Y and Z atom occupy the B and D atomic sites, respectively. If ξ , η or ζ impurity can substitute predominantly X, Y or Z atom, respectively and such a substitution occurs independently, we can obtain the following three kind of alloy systems $HA(\xi)$, $HA(\eta)$ and $HA(\zeta)$.

$$HA(\xi) = (X_{1-v} \xi_v)_2YZ, \quad HA(\eta) = X_2(Y_{1-v} \eta_v)Z, \quad HA(\zeta) = X_2Y(Z_{1-v} \zeta_v) \quad (1)$$

where v is the fraction of the impurity in its predominant atomic site. Putting, for example, $\eta = Z$, one may treat a quasi-binary system in the same scheme.

In Table 2, the constitution of the j -th neighbouring atomic shell indicated by the kind of atom W (its atomic site S) and its number $n_j(W)$ are described for X, Y and Z central atoms in the ordered and stoichiometric alloy X_2YZ . In an alloy containing the impurity q such as $HA(q)$, then only the atomic shells with the particular atomic site S are influenced so as to have the impurity q . Such an atomic shell is called an impurity shell hereafter. Then, the local environment expressing the effect of the impurity on the central atom may be described by a series of the number of impurities $\{n_j(q)\}$ in these impurity shells surrounding the central atom $W = X, Y$ or Z . This set of the number of the impurity is represented by \hat{q}_W and is called environment variable hereafter.

By the aid of Table 2, the environment variables for X, Y, Z and the impurity q itself are easily obtained and given in Table 3 for three type alloys $HA(\xi)$, $HA(\eta)$ and $HA(\zeta)$, respectively.

After such a procedure, an atom W ($=X, Y, Z, \xi, \eta$ or ζ) in these

Table 2. Constitution of each atomic shell in X_2YZ Heusler alloy for X, Y and Z central atom respectively.

Center atom Shell No.	X	Y	Z
0	X(A,C)	Y(B)	Z(D)
1	4Y(B), 4Z(D)	8X(A,C)	8X(A,C)
2	6X(A,C)	6Z(D)	6Y(B)
3	12X(A,C)	12Y(B)	12Z(D)
4	12Y(B), 12Z(D)	24X(A,C)	24X(A,C)
5	8X(A,C)	8Z(D)	8Y(B)
6	6X(A,C)	6Y(B)	6Z(D)
7	12Y(B), 12Z(D)	24X(A,C)	24X(A,C)
8	24X(A,C)	24Z(D)	24Y(B)
9	24X(A,C)	24Y(B)	24Z(D)
10	12Y(B), 12Z(D)	24X(A,C)	24X(A,C)
10'	4Y(B), 4Z(D)	8X(A,C)	8X(A,C)
11	12X(A,C)	12Y(B)	12Z(D)
12	24Y(B), 24Z(D)	48X(A,C)	48X(A,C)
13	6X(A,C)	6Z(D)	6Y(B)
13'	24X(A,C)	24Z(D)	24Y(B)
14	24X(A,C)	24Y(B)	24Z(D)
15	12Y(B), 12Z(D)	24X(A,C)	24X(A,C)

three type alloys is specified by the environment variable \hat{q}_W , such as $W_S = (W, \hat{q}_W)$, where W_S means the atom W in the alloy containing impurity q occupying S atomic site predominantly and $\hat{q}_W = \{n_j(q)\} = [n_{1S}(q), n_{2S}(q), \dots]$ as shown in Table 3. Clearly $n_j(q)$ is an integer variable from zero to $s_j(q) = n_j(q)_{\max}$, which is easily obtained in Table 2, putting $s_j(q) = n_j(S)$. In the right side of Table 3, $\hat{q}_W(\max) = \{s_j(q)\}$ is also given for convenience.

Since the nearest neighbour impurity q must have the stronger effect on the central atom W than more outer impurities, $n_j(q) = n_{1S}(q)$ with the least j in each \hat{q}_W is the most important component in the environment variable. In fact the corresponding $s_j(q)$ gives the maximum number of satellites permitted for the actual NMR spectrum as can be seen in later.

III. Fundamental Equations and Moment Representation

In general the hyperfine field of a nucleus is expressed in two terms, namely the one is supplied from the central atom containing the nucleus itself and the others from the neighbouring atoms as follows,

$$H_{hf}(W, \hat{q}_W) = H_0(W) \mu(W, \hat{q}_W) + \sum_{iu} \sum H_i(W) \mu_u^M(W, \hat{q}_W)_i^U \quad (2)$$

Table 3. The environment variable $\hat{q}_W = \{n_j(q)\}$ for W atom in three kind of Heusler alloys HA(ξ), HA(η) and HA(ζ), when the impurity $q = \xi, \eta$ and ζ respectively. $\hat{q}_W(\max) = \{s_j(q)\}$, where $s_j(q) = n_j(q)_{\max}$.

$HA(\xi) = (X_{1-v}\xi_v)_2YZ$	
$\xi_X = [n_2(\xi), n_3(\xi), n_5(\xi), n_6(\xi), \dots]$	$\xi_X(\max) = [6, 12, 8, 6, \dots]$
$\xi_\xi = [n_0, n_2(\xi), n_3(\xi), n_5(\xi), n_6(\xi), \dots]$	$\xi_\xi(\max) = [1, 6, 12, 8, 6, \dots]$
$\xi_Y = [n_1(\xi), n_4(\xi), n_7(\xi), n_{10}(\xi), \dots]$	$\xi_Y(\max) = [8, 24, 24, 24, \dots]$
$\xi_Z = [n_1(\xi), n_4(\xi), n_7(\xi), n_{10}(\xi), \dots]$	$\xi_Z(\max) = [8, 24, 24, 24, \dots]$
$HA(\eta) = X_2(Y_{1-v}\eta_v)Z$	
$\hat{\eta}_X = [n_1(\eta), n_4(\eta), n_7(\eta), n_{10}(\eta), \dots]$	$\hat{\eta}_X(\max) = [4, 12, 12, 12, \dots]$
$\hat{\eta}_Y = [n_3(\eta), n_6(\eta), n_9(\eta), n_{11}(\eta), \dots]$	$\hat{\eta}_Y(\max) = [12, 6, 24, 12, \dots]$
$\hat{\eta} = [n_0, n_3(\eta), n_6(\eta), n_9(\eta), n_{11}(\eta), \dots]$	$\hat{\eta}_\eta(\max) = [1, 12, 6, 24, 12, \dots]$
$\hat{\eta}_Z = [n_2(\eta), n_5(\eta), n_8(\eta), n_{13}(\eta), \dots]$	$\hat{\eta}_Z(\max) = [6, 8, 24, 6, \dots]$
$HA(\zeta) = X_2Y(Z_{1-v}\zeta_v)$	
$\zeta_X = [n_1(\zeta), n_4(\zeta), n_7(\zeta), n_{10}(\zeta), \dots]$	$\zeta_X(\max) = [4, 12, 12, 12, \dots]$
$\zeta_Y = [n_2(\zeta), n_5(\zeta), n_8(\zeta), n_{13}(\zeta), \dots]$	$\zeta_Y(\max) = [6, 8, 24, 6, \dots]$
$\zeta_Z = [n_3(\zeta), n_6(\zeta), n_9(\zeta), n_{11}(\zeta), \dots]$	$\zeta_Z(\max) = [12, 6, 24, 12, \dots]$
$\zeta_\zeta = [n_0, n_3(\zeta), n_6(\zeta), n_9(\zeta), n_{11}(\zeta), \dots]$	$\zeta_\zeta(\max) = [1, 12, 6, 24, 12, \dots]$

where it must be noted that the nucleus is characterized not only W atom containing the nucleus but also by its environment variable \hat{q}_W . $H_0(W)$ and $H_i(W)_U$ are the hyperfine field coefficients. $\mu(W, \hat{q}_W)$ and $M(W, \hat{q}_W)_i^U$ are the atomic moment of the central atom W and the partial shell moment consisting of U atoms in the i-th atomic shell, respectively.

Essentially the hyperfine field $H_{hf}(W, \hat{q}_W)$ is produced by the δ function type interaction between the moment of nucleus and the polarized s electrons occupying the position of the nucleus. Since the s electron polarization in turn is caused by the outer electron polarization, especially by d like electrons, the atomic moment and shell moment play the fundamental role in the hyperfine field as shown in Eq. (2). The effect of the outer atomic shell moment may be transferred through the 4s like itinerant electron, of which the polarization is determined at the outer atomic shell in turn. Therefore, the hyperfine field coefficient $H_i(W)_U$ is characterized also by U in addition to W.

In a simple first neighbour approximation for the hyperfine

interaction from the outer shell moments, Eq.(2) is reduced to,

$$H_{hf}(W_S) = H_0(W) \mu(W_S) + \sum_u H_{1u}(W) M(W_S)_1^U \quad (2)'$$

where an abbreviation such as $W_S = W, \hat{q}_W$ is used for simplification. Clearly the environment effect on $H_{hf}(W_S)$ is only expected through the atomic moment $\mu(W_S)$ and $M(W_S)_1^U$ in Eq.(2)'. Therefore, we must consider and find the environment effect upon these moments.

Regarding the environment effect upon the atomic moment, many workers, for example, Beck¹³⁾ have proposed a linear variation of the moment with the number of a certain kind of atom in the 1st neighbour around the atom concerned. And Niculescu et al.⁶⁾ combined ingeniously this effect with the hyperfine field as described in Introduction.

At present work, in a similar but more general way the environment effect upon the moment will be defined by the aid of several phenomenological coefficients and simultaneously with a consideration of the induced moment effect.

We assume that the moment of W atom consists of two parts, namely the bond character moment $\mu_P(W_S)$ and the induced moment $\mu(W_S)'$. For simplification, it is assumed that all the magnetic moments arrange perfectly at the absolute zero temperature and therefore $\mu(W_S)'$ is simply proportional to the 1st atomic shell moment $M(W_S)_1^U$ as follows,

$$\mu(W_S)' = \mu(W_S) - \mu_P(W_S) = \sum_u K(WU) M(W_S)_1^U \quad (3)$$

while $\mu_P(W_S)$ is assumed to have the following expression, which is compatible with the conventional model described above^{6),13)}.

$$\mu_P(W_S) = \sum_u J(WU) [n_1(U)/n_1] \quad (3)'$$

where

$$n_1 = \sum_u n_1(U) \quad (3)''$$

The phenomenological coefficients $J(WU)$ and $K(WU)$ may be called the bond character moment coefficient and the induced moment coefficient, respectively. $K(WU)$ may be understood as a product $\chi(W)C(WU)$, where $\chi(W)$ is a kind of atomic susceptibility and $C(WU)$ a molecular field coefficient arising from the interatomic exchange interaction. While $J(WU)$ may be originated together from the character of the bonding and antibonding orbitals of W atom under an influence of the outer U atom and the intra-atomic exchange interaction within itself.

If these expressions of moments are permitted, all the matter will be developed easily in a formal way. At first it is pointed out that the 1st atomic shell moment may be expressed in turn in terms of its related atomic shell moments. A related atomic shell of the 1st

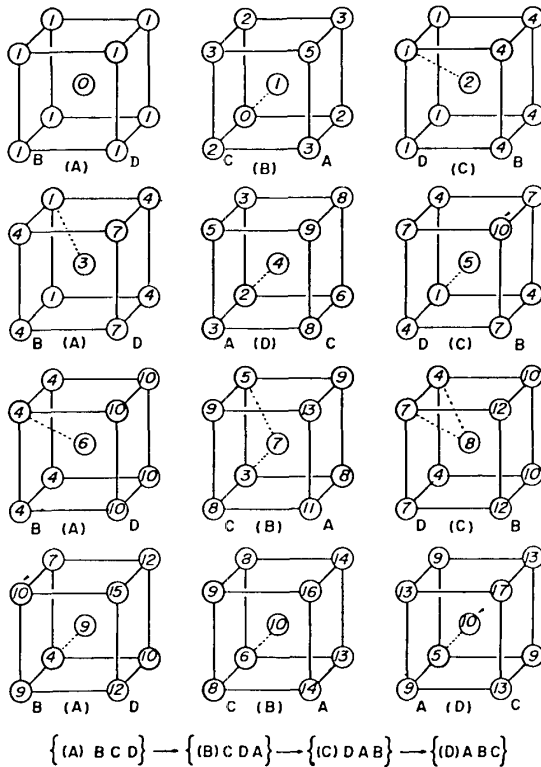


Fig. 3. The arrangement of the 1st neighbour atom with its shell number around a central atom belonging to the j -th atomic shell for $j=0 \sim 10$. The atomic site of each central atom and those of its neighbour atoms are indicated with and without parenthesis.

The cyclic relation given in the bottom shows the variation of the assignment of the atomic sites, when the central atomic site is altered from A to B, C and D.

atomic shell is defined as the atomic shell consisting of only the atoms in the actual first neighbours around an atom belonging to the original 1st atomic shell of the central atom W . As can be seen in Fig. 3, the related atomic shells of the 1st atomic shell are the 0 (i. e. the central atom), 2nd, 3rd and 5th atomic shells and therefore the 1st atomic shell moment is expressed in terms of these shell moments by the aid of Eqs. (3) and (3)' as follows,

$$\begin{aligned}
 M(W_S)_1^U &= n_1(U) \mu_P(U_S)_1 \\
 &+ [n_1(U)/n_1] \sum_j m_{j1} [K(UT)M(W_S)_j^T + K(UV)M(W_S)_j^V \\
 &+ K(Uq)M(W_S)_j^q] \quad (4)
 \end{aligned}$$

$$\begin{aligned}
 \mu_P(U_S)_1 &= (1/n_1)^2 \sum_j m_{j1} [n_j(T)J(UT) + n_j(V)J(UV) + n_j(q)J(Uq)] \\
 &= (1/n_1)^2 \sum_j m_{j1} \{ (1/2)n_j [J(UT) + J(UV)] + n_j(q) [J(Uq) - J(UT)] \} \quad (4)'
 \end{aligned}$$

where m_{j1} is the number of atoms belonging to the 1st atomic shell around an atom of its related shell with the shell number j . Paying an attention to the unit bcc lattice having the central atom with the number $j=0, 2, 3$ and 5 in Fig. 3, one may obtain $m_{01}=8$, $m_{21}=4$, m_{31}

= 2 and $m_{51} = 1$.

Clearly $M(W_S)_1^U$ is also composed of the bond character moments and the induced moments produced by its related shell moments. In some shells, $T = V$ or $n_j(q) = 0$ relation is realized. It must be emphasized that $\mu(W_S)$ is dependent on the environment variable through $n_j(q)$ or $n_1(U)$, if $U = q$, as can be seen in Eqs.(3) ~ (4)'.

In a similar way, we may obtain the similar expressions for $M(W_S)_2^U$, $M(W_S)_3^U$ and so forth, which may be expressed in terms of atomic shell moments far apart from the central atom with increasing j . In such a procedure up to the m -th shell, we may have t relations concerning $\mu(W_S)$, $M(W_S)_1^U, \dots, M(W_S)_m^U$, where t is dependent on m as well as q . Then, from the definition and taking into account the successive decreasing of the impurity effect upon the central atom, when the impurity is far apart from the central atom, one may put the following two relations,

$$M(W_S)_0 = M(W_S)_0^W = \mu(W_S) \quad (5)$$

$$M(W_S)_j^U = n_j(U) \overline{\mu(U_S)} \quad ; \quad j \geq m+1 \quad (5)'$$

Then, the simultaneous linear equations for $\mu(W_S)$ and $M(W_S)_j^U$; ($j \leq m$) are obtained and they are solved as functions of atomic average moment $\overline{\mu(W_S)}$ and the environment variable $\hat{q}_W = \{n_j(q)\}$ together with $J(WU)$ and $K(WU)$ coefficients. An example of the simultaneous equation will be given in the next section.

In the final of this section, we give the population $p(W_S) = p(W, \hat{q}_W)$ of the atom W characterized by its environment variable $\hat{q}_W = \{n_j(q)\}$. This is easily performed in the conventional manner^{6), 13)} by the aid of the binominal distribution function, namely,

$$p(W_S) = p(W, \hat{q}_W) = c(W) \prod_j p(n_j(q), s_j(q)) \quad (6)$$

$$p(n, s) = {}_s C_n (1-v)^{s-n} v^n \quad (6)'$$

where $c(W)$ is the atomic fraction of W atom and is obtained from Eq. (1) as a function of v .

The sum of $p(W_S)$ in respect of \hat{q}_W and W is equal to unity and therefore $p(W_S)$ plays a role of the probability function of any physical quantity in the alloy $HA(q)$. $\overline{\mu(W_S)}$ used in Eq.(5)' is also defined by this function as follows,

$$\overline{\mu(W_S)} = \sum_{q_W} p(W_S) \mu(W_S) / c(W) \quad (7)$$

The intensity of the NMR resonance peak is supposed to be directly proportional to the population of the resonating nucleus and thus

is given in the following expression,

$$I(W_S) = I(W, \hat{q}_W) = k(W) p(W_W) \quad (8)$$

where $k(W)$ is the weighting factor of the intensity of W nucleus. It may be ascribed to its natural abundance etc. and determined experimentally but may be constant through the same alloy system irrespective of the alloy composition as well as the environment variable \hat{q}_W .

IV. Simultaneous Linear Equation for Moments, their Solution and Hyperfine Field

1. Simultaneous equation and moment expression

According to the previous section, we can obtain the simultaneous linear equation for moments. An example of the equations for the moment of X atom characterized by the environment variable $\hat{n}_X = [n_1(\eta), n_4(\eta), n_7(\eta), \dots]$ in $HA(\eta)$ alloy is described in the following, when the chain of the interaction is cut at $m=1$.

$$\begin{aligned} \mu(X_B) - K(XY)M(X_B)_1^Y - K(X_B)M(X_B)_1^\eta - K(XZ)M(X_B)_1^Z &= (1/2) [J(XY) + J(XZ)] \\ &+ [n_1(\eta)/8] [J(X\eta) - J(XY)] \\ - [4 - n_1(\eta)] K(YX) \mu(X_B) + M(X_B)_1^Y &= [4 - n_1(\eta)] [J(YX) + 7K(YX) \overline{\mu(X_B)}] \\ - n_1(\eta) K(\eta X) \mu(X_B) + M(X_B)_1^\eta &= n_1(\eta) [J(\eta X) + 7K(\eta X) \overline{\mu(X_B)}] \\ - 4K(ZX) \mu(X_B) + M(X_B)_1^Z &= 4 [J(ZX) + 7K(ZX) \overline{\mu(X_B)}] \end{aligned}$$

Clearly the solutions for $\mu(X_B)$, $M(X_B)_1^Y$, $M(X_B)_1^\eta$ and $M(X_B)_1^Z$ are functions of the component of the environment variable $n_1(\eta)$ and atomic average moment $\overline{\mu(X_B)}$ together with $J(WU)$ and $K(WU)$ coefficients. Other equations and solutions have also similar form and character.

Since the exact solutions are rather lengthy, all the results on the moments are given in the first order of $K(WU)$. Then, for the alloy $HA(\eta) = X_2(Y_{1-\nu}n_\nu)Z$, the atomic moments are,

$$\begin{aligned} \mu(X_B) &= \mu_0(X) + (1/4) \delta n_1(\eta) \\ \mu(Y_B) &= \mu_0(Y) + (1/2) K(YX) \delta n_3(\eta) \\ \mu(\eta_B) &= \mu_0(\eta) + (1/2) K(\eta X) \delta n_3(\eta) \\ \mu(Z_B) &= \mu_0(Z) + (1/4) \delta [4n_2(\eta) + n_5(\eta)] \end{aligned} \quad (9)$$

and for the stoichiometric alloy X_2YZ ,

$$\begin{aligned}
\mu_0(X) &= \mu_0^0(X) + 4K(KJ)_0, & \mu_0^0(X) &= J_0 \\
\mu_0(Y) &= \mu_0^0(Y) + 8K(YX)\mu_0(X), & \mu_0^0(Y) &= J(YX) \\
\mu_0(\eta) &= \mu_0^0(\eta) + 8K(\eta X) [\mu_0(X) + (\delta/4)], & \mu_0^0(\eta) &= J(\eta X) \\
\mu_0(Z) &= \mu_0^0(Z) + 8K(ZX)\mu_0(X), & \mu_0^0(Z) &= J(ZX)
\end{aligned} \tag{10}$$

$$\text{where, } 2J_0 = J(XY) + J(XZ), \quad (KJ)_0 = K(XY)J(YX) + K(XZ)J(ZX) \tag{11}$$

$$2\delta = 2J_1 + 8[K(X\eta)J(\eta X) - K(XY)J(YX)], \quad 2J_1 = J(X\eta) - J(XY) \tag{12}$$

In these expressions the quantity of the stoichiometric alloy is expressed with the lower suffix "0" such as $\mu_0(X)$. $\mu_0^0(X)$ means the moment of $\mu_0(X)$, when all $K(WU)$ coefficients are zero. The same notation will be used hereafter.

In a similar way, the 1st shell moments are described as follows,

$$\begin{aligned}
M(X_B)_1^Y &= M_0(X)_1^Y + 28K(YX) [\overline{\mu(X_B)} - \mu_0(X)] - [\mu_0(Y) - K(YX)\delta] n_1(\eta) \\
&\quad - (1/4)K(YX)\delta n_1(\eta)^2 \\
M(X_B)_1^\eta &= \mu_0(\eta)n_1(\eta) - 2K(\eta X)\delta n_1(\eta) + (1/4)K(\eta X)\delta n_1(\eta)^2 \\
M(X_B)_1^Z &= M_0(X)_1^Z + 28K(ZX) [\overline{\mu(X_B)} - \mu_0(X)] + K(ZX)\delta n_1(\eta) \\
M(Y_B)_1^X &= M_0(Y)_1^X + 24K(XY) [\overline{\mu(Y_B)} - \mu_0(Y)] + 32[\overline{\mu(Z_B)} - \mu_0(Z)] \\
&\quad + (1/2)\delta n_3(\eta) \\
M(\eta_B)_1^X &= M_0(\eta)_1^X + 24K(XY) [\overline{\mu(Y_B)} - \mu_0(Y)] + 32K(XZ) [\overline{\mu(Z_B)} - \mu_0(Z)] \\
&\quad + (1/2)\delta n_3(\eta) \\
M(Z_B)_1^X &= M_0(Z)_1^X + 24K(XZ) [\overline{\mu(Z_B)} - \mu_0(Z)] + 32K(XY) [\overline{\mu(Y_B)} - \mu_0(Y)] \\
&\quad + (1/4)\delta [4n_2(\eta) + n_5(\eta)]
\end{aligned} \tag{13}$$

$$\begin{aligned}
M_0(X)_1^Y &= 4\mu_0(Y), & M_0(X)_1^Z &= 4\mu_0(Z) \\
M_0(Y)_1^X &= M_0(Z)_1^X = 8\mu_0(X) \\
M_0(\eta)_1^X &= 8[\mu_0(X) + (\delta/4)]
\end{aligned} \tag{14}$$

In these moment expressions, it must be emphasized that the bond character moments play the most important role in the magnetism of an alloy. If there is no nonvanishing $\mu_0^0(W)$ or J_1 , the alloy could not

be magnetic and shows constant paramagnetism. On the contrary, any atom with a finite bond character moment can produce some induced moment on all other atoms in this Heusler alloy system. Therefore, we call the atom W with nonvanishing $\mu_0^0(W)$ magnetic and η atom capable to contribute a finite $J(X\eta)$ an active impurity hereafter.

2. Hyperfine field

From the above results, we can easily obtain the hyperfine field according to Eq. (2)'.
 For the stoichiometric alloy X_2YZ ,

$$H_{\text{hf}}(X)_0 = H_0(X)\mu_0(X) + 4[H_1(X)_Y\mu_0(Y) + H_1(X)_Z\mu_0(Z)] \quad (15)$$

$$= [H_0(X) + 32\theta(X)_{YZ}]\mu_0(X) + 4[H_1(X)_X\mu_0^0(Y) + H_1(X)_Z\mu_0^0(Z)]$$

$$H_{\text{hf}}(Y)_0 = H_0(Y)\mu_0(Y) + 8H_1(Y)_X\mu_0(X) \quad (16)$$

$$= H_0(Y)\mu_0^0(Y) + 8\epsilon(Y)_X\mu_0(X)$$

$$H_{\text{hf}}(\eta)_0 = H_0(\eta)\mu_0(\eta) + 8H_1(\eta)_X[\mu_0(X) + (\delta/4)] \quad (17)$$

$$= H_0(\eta)\mu_0^0(\eta) + 8\epsilon(\eta)_X[\mu_0(X) + (\delta/4)]$$

$$H_{\text{hf}}(Z)_0 = H_0(Z)\mu_0(Z) + 8H_1(Z)_X\mu_0(X) \quad (18)$$

$$= H_0(Z)\mu_0^0(Z) + 8\epsilon(Z)_X\mu_0(X)$$

where

$$\theta(X)_{YZ} = H_1(X)_Y K(YX) + H_1(X)_Z K(ZX) \quad (19)$$

$$\epsilon(W)_X = H_1(W)_X + H_0(W)K(WX) ; W = Y, \eta, Z \quad (20)$$

For the HA(η) = $X_2(Y_{1-\nu}\eta_\nu)Z$ alloy,

$$H_{\text{hf}}(X_B) = H_{\text{hf}}(X)_0 + B(X_B)[\overline{\mu(X_B)} - \mu_0(X)] + C_1(X_B)n_1(\eta) + C_2(X_B)n_1(\eta)^2 \quad (15)'$$

$$H_{\text{hf}}(Y_B) = H_{\text{hf}}(Y)_0 + B_1(Y_B)[\overline{\mu(Y_B)} - \mu_0(Y)] + B_2(Y_B)[\overline{\mu(Z_B)} - \mu_0(Z)] + C(Y_B)n_3(\eta) \quad (16)'$$

$$H_{\text{hf}}(\eta_B) = H_{\text{hf}}(\eta)_0 + B_1(\eta_B)[\overline{\mu(Y_B)} - \mu_0(Y)] + B_2(\eta_B)[\overline{\mu(Z_B)} - \mu_0(Z)] + C(\eta_B)n_3(\eta) \quad (17)'$$

$$H_{\text{hf}}(Z_B) = H_{\text{HF}}(Z)_0 + B_1(Z_B)[\overline{\mu(Z_B)} - \mu_0(Z)] + B_2(Z_B)[\overline{\mu(Y_B)} - \mu_0(Y)] + C(Z_B)[4n_2(\eta) + n_5(\eta)] \quad (18)'$$

where the related parameters $B_j(W)$ and $C_j(W)$ are given as follows,

$$\begin{aligned}
B(X_B) &= 28\theta(X)_{yz} \\
C_1(X_B) &= (1/4)H_0(X)\delta + H_1(\eta)_{x\mu_0}(\eta) - H_1(Y)_{x\mu_0}(Y) \\
&\quad + [\theta(X)_{yz} - 2H_1(X)_{\eta}K(\eta X)]\delta
\end{aligned} \tag{15}''$$

$$\begin{aligned}
C_2(X_B) &= (1/4)[K(\eta X) - K(YX)]\delta \\
B_1(Y_B) &= 24K(XY)\epsilon(Y)_x, \quad B_2(Y_B) = 32K(XZ)\epsilon(Y)_x \\
C(Y_B) &= (1/2)\epsilon(Y)_x\delta
\end{aligned} \tag{16}''$$

$$\begin{aligned}
B_1(\eta_B) &= 24K(XY)\epsilon(\eta)_x, \quad B_2(\eta_B) = 32K(XZ)\epsilon(\eta)_x \\
C(\eta_B) &= (1/2)\epsilon(\eta)_x\delta
\end{aligned} \tag{17}''$$

$$\begin{aligned}
B_1(Z_B) &= 24K(XZ)\epsilon(Z)_x, \quad B_2(Z_B) = 32K(XY)\epsilon(Z)_x \\
C(Z_B) &= (1/4)\epsilon(Z)_x\delta
\end{aligned} \tag{18}''$$

In the expression for the stoichiometric alloy X_2YZ , one may easily find that it consists of two parts, namely the self hyperfine interaction and the 1st neighbour hyperfine interaction. It will be shown in the next section that the latter is comparable with the former in some cases.

In the hyperfine field expression of the alloy $HA(\eta)$ containing the impurity η , two additional terms are recognized besides the term of the stoichiometric alloy. They are the composition dependent term with the factor $\overline{\mu(W_B)} - \mu_0(W)$ and the $n_j(\eta)$ dependent term. In the NMR spectrum of $HA(\eta)$ alloy, the stoichiometric term corresponds to the main peak of the resonance spectrum, the composition dependent term to the shift of the resonance peaks with alloying and the $n_j(\eta)$ dependent term to the satellite peaks.

In fact the last one is the origin of the occurrence of satellite peaks of the NMR spectrum and determines the separation between two adjacent satellite peaks. As can be seen in Eqs. (15)' ~ (18)', the component of the environment variable \hat{q}_W , which causes the occurrence of the satellite peaks, varies with the central atom containing the resonating nucleus; $n_1(\eta)$, $n_3(\eta)$, $n_3(\eta)$ and $n_2(\eta)$ to X, Y, η and Z, respectively, as already appointed by Niculescu et al.⁶⁾. Each of these component is that with the least j in each environment variable in Table 3 and therefore its maximum corresponds to the maximum available number of satellites.

As to the parameters $H_{hf}(W)_0$, $B_j(W_B)$ and $C_j(W_B)$ that determine

the main peak position, peak shift and satellite separation, it must be mentioned that they are all expressed in terms of the phenomenological coefficients $H_0(W)$, $H_1(W)_u$, $K(W,U)$ and the moments $\mu_0(W)$ and δ that are obtainable directly from experiments. Because $J(WU)$ coefficients are replaced by $\mu_0(W)$ and δ by the aid of the simultaneous equations for the stoichiometric alloy. This fact is helpful to the analysis of the experiments as described in later.

3. Atomic average moment

According to Eqs. (6) and (7), the atomic average moments are easily obtained as follows,

$$\begin{aligned}\overline{\mu(X_B)} &= \mu_0(X) + \delta v \\ \overline{\mu(Y_B)} &= \mu_0(Y) + 6K(YX)\delta v \\ \overline{\mu(\eta_B)} &= \mu_0(\eta) + 6K(\eta X)\delta v \\ \overline{\mu(Z_B)} &= \mu_0(Z) + 8K(ZX)\delta v\end{aligned}\tag{21}$$

These expressions assure the possibility to determine δ , which is necessary to analyze the hyperfine field. Furthermore, it is to be noted that δ is certainly measurable, if there is any appreciable change in the hyperfine field by alloying. Because the satellite term of the hyperfine field is almost proportional to δ in any case as can be seen in Eqs. (15) ~ (18).

4. Comparison with Niculescu et al.'s idea

If we imagine that all $K(WU)$ coefficients are zero, then the obtained results should correspond to the results by Niculescu et al.⁶⁾. Even in such a case, however, there is an important difference between the present model and theirs. They noticed that the impurity effect upon the atomic moment of X in A,C site, which in turn affect the hyperfine field of X, Y, η and Z atoms but did not dare to use the observed moment of $\mu_0(X)$, $\mu_0(Y)$, $\mu_0(\eta)$ and δ as the important parameters to analyze the experiments. Instead they used a hypothetical relation between the moment of X and the number of Y atoms in the 1st neighbour of X to analyze the NMR spectrum. This indirect relation made them to fail to find several important relations obtained experimentally, such as the relation between the $\delta/\mu_0(X)$ and $C(W)_B/H_{hf}(W)_0$, which is easily obtained in the present model, as described in later.

Furthermore, in the present model we can interpret the shift of the resonance peaks with alloying by introducing the induced moment effect, which is observed by them but is not interpreted. The induced

moment effect should be necessary in the phenomenological approach to the hyperfine field to interpret the nonvanishing value of $H_{hf}(Z)_0$ in the case of X_2YZ with nonmagnetic X element. This is one of the most interesting problems of the NMR study in Heusler alloys and many workers have tried to interpret it¹⁴⁾. In the present model, $H_{hf}(Z)_0$ is able to be finite through Eqs.(10), (11) and (18), while it vanishes when one stops in the same step as Niculescu et al.⁶⁾. In spite of such a weakness, their idear is a very progressive one as already described in Introduction.

V. Determination of Phenomenological Coefficients

In the present hyperfine field expressions and the atomic average moment ones, we have 13 relations for fields and four for moments in a single HA(η) alloy system as described in Eqs.(15) ~ (20). In these expressions ten hyperfine field coefficients (four for $H_0(W)$, three for $H_1(W)_x$ and three for $H_1(X)_w$) and six induced moment coefficients (three for K(WX) and three for K(XW)) are to be determined.

Though 17 relations are enough to determine 16 coefficients, it is difficult to obtain in practice the hyperfine fields of all the nuclei because of the lack of the natural abundance of some of them and also to determine precisely the composition dependence of $\overline{\mu(W_B)}$ for $W= Y, \eta$ and Z .

Therefore, several ratios of the hyperfine field to the moment, which is useful to the analysis of the NMR spectrum, are given in the following.

(1) For the main peak of NMR in X_2YZ and HA(η) alloys

When X and W are magnetic, $W= Y$ or η

$$\alpha(X)_{YZ} = H_{hf}(X)_0/\mu_0(X) = H_0(X) + 4H_1(X)_Y [\mu_0(Y)/\mu_0(X)] + 32H_1(X)_Z K(ZX) \quad (22)$$

$$\beta(Y)_x = H_{hf}(Y)_0/\mu_0(Y) = H_0(Y) + 8H_1(Y)_x [\mu_0(X)/\mu_0(Y)] \quad (23)$$

$$\beta(\eta)_x = H_{hf}(\eta)_0/\mu_0(\eta) = H_0(\eta) + 8H_1(\eta)_x \{ [\mu_0(X) + (\delta/4)]/\mu_0(\eta) \} \quad (24)$$

When X is magnetic but W is nonmagnetic, $W= Y, \eta$ or Z

$$\epsilon(Y)_x = H_{hf}(Y)_0/8\mu_0(X) = H_1(Y)_x + H_0(Y)K(YX) \quad (25)$$

$$\epsilon(\eta)_x = H_{hf}(\eta)_0/8[\mu_0(X) + (\delta/4)] = H_1(\eta)_x + H_0(\eta)K(\eta X) \quad (26)$$

$$\epsilon(Z)_x = H_{hf}(Z)_0/8\mu_0(X) = H_1(Z)_x + H_0(Z)K(ZX) \quad (27)$$

When X is nonmagnetic but Y is magnetic

$$\beta(Y)_x^* = H_{hf}(Y)_0 / \mu_0(Y) = H_0(Y) + 32H_1(Y)_x K(XY) \quad (28)$$

$$\epsilon(X)_Y = H_{hf}(X)_0 / 4\mu_0(Y) = H_1(X)_Y + H_0(X) K(XY) \quad (29)$$

$$\gamma(Z)_{xy} = H_{hf}(Z)_0 / 32\mu_0(Y) = H_1(Z)_x K(XY) \quad (30)$$

(2) For the satellite peak of NMR in HA(η) alloy

$$\theta(X)_{yz} = B(X_B) / 28 = H_1(X)_Y K(YX) + H_1(X)_Z K(ZX) \quad (31)$$

$$\rho(X)_{\eta z} = 4C_1(X_B) / \delta = H_0(X) - 4H_1(Y)_x [\mu_0(Y) / \delta] \\ + 4H_1(\eta)_x [\mu_0(\eta) / \delta] + O(K) \quad (32)$$

$$O(K) = 4[\theta(X)_{yz} - 2H_1(X)_\eta K(\eta X)] \quad (32)'$$

$$\epsilon(Y)_x = 2C(Y_B) / \delta = H_1(Y)_x + H_0(Y) K(YX) \quad (25)'$$

$$\epsilon(\eta)_x = 2C(\eta_B) / \delta = H_1(\eta)_x + H_0(\eta) K(\eta X) \quad (26)'$$

$$\epsilon(Z)_x = 4C(Z_B) / \delta = H_1(Z)_x + H_0(Z) K(ZX) \quad (27)'$$

Regarding the application of these ratios to the analysis of NMR spectrum, the following technique may be mentioned.

- (a) When both X and Y are magnetic in X_2YZ , $H_0(Y)$ and $H_1(Y)_x$ may be obtained from a series of observation of $H_{hf}(Y)_0$, $\mu_0(X)$ and $\mu_0(Y)$ in the alloys with the same X and Y but different Z elements according to Eq. (23).
- (b) If $K(ZX)$ is assumed very small, $H_0(X)$ and $H_1(X)_Y$ are also obtained in a similar way as above according to Eq. (22).
- (c) When both X and Y are magnetic in HA(η) alloy system, $H_0(Y)$ and $H_1(Y)_x$ are obtained from $H_{hf}(Y)_0$, $\mu_0(X)$, $\mu_0(Y)$, δ and $C(Y_B)$, on an assumption $H_1(Y)_x = \epsilon(Y)_x$, according to Eqs. (23) and (25)'
- (d) When both X and η are magnetic in HA(η) alloy system, $H_0(\eta)$ and $H_1(\eta)_x$ are obtained in a similar way as above according to Eqs. (24) and (26)'
- (e) When X is magnetic but W (=Y, η or Z) is nonmagnetic in HA(η) alloy system, $\epsilon(W)_x$ is obtained independently either from $H_{hf}(W)_0 / \mu_0(X)$ or from $C(W_B) / \delta$ according to Eqs. (25) ~ (27) and (25)' ~ (27)'. In such a case, two values of $\epsilon(W)_x$ from different sources should be equal giving the following relation.

$$\delta / \mu_0(X) = 16C(Y_B) / H_{hf}(Y)_0 = 32C(Z_B) / H_{hf}(Z)_0 \quad (33)$$

$$\delta / [\mu_0(X) + (\delta/4)] = 16C(\eta_B) / H_{hf}(\eta)_0 \quad (33)'$$

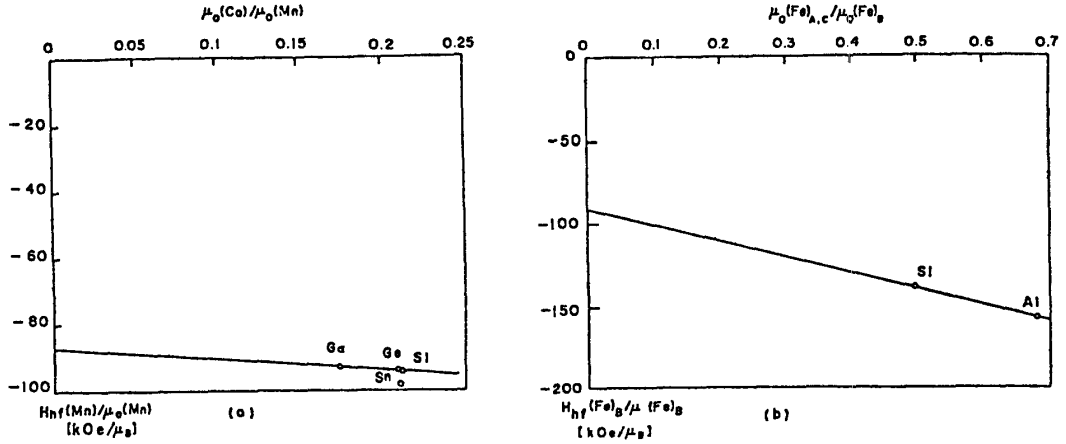


Fig. 4. Determination of $H_0(Y)$ and $H_1(Y)_x$ according to the relation $\beta(Y)_x = H_0(Y) + 8H_1(Y)_x [\mu_0(X)/\mu_0(Y)]$, where $\beta(Y)_x = H_{hf}(Y)_0/\mu_0(Y)$. (a) Co_2MnZ (ref. to (15)~(17)) and (b) Fe_3Z (ref. to (10)).

In the next section, we will apply these techniques to the analysis of several NMR experiments to obtain the $H_0(W)$ and $H_1(W)_x$ coefficients.

VI. Comparison with Experiments

1. Stoichiometric alloys and determination of $H_0(Y)$

Since both X and Y are magnetic in Co_2MnZ ¹⁵⁾ and Fe_3Z ¹⁰⁾ alloy systems and the hyperfine field measurements have been also performed in these systems^{10),16),17)}, the technique (a) is applicable to these systems. In Fig. 4, by applying the linear relation to the $H_{hf}(Y)_0/\mu_0(Y)$ vs $\mu_0(X)/\mu_0(Y)$ plot, one may obtain $H_0(Mn) = -86.57$ and $H_1(Mn)_{Co} = -4.66$ [kOe/μ_B] in (a) and $H_0(Fe) = -90.19$ and $H_1(Fe)_{Fe} = -12.25$ [kOe/μ_B] in (b).

In Fe_3Z alloy system, the obtained coefficients may be applied immediately to estimate $H_{hf}(Fe)_0$ in A,C sites according to Eq. (22) and on an assumption of small $K(ZX)$. The calculated value is equal to -236.54 for Fe_3Al and -225.83 [kOe/μ_B] for Fe_3Si . While the experimental value is -246 for Fe_3Al and -222 [kOe/μ_B] for Fe_3Si ¹⁰⁾. The agreement between the experimental and the calculated is fairly well and seems to give a support to the present model.

2. Off-stoichiometric $Fe_{3-x}V_xSi$ alloy

In this alloy system, the detailed NMR spectrum has been obtained

Table 4. The hyperfine field, atomic moment and their related parameters in $\text{Fe}_{3-x}\text{V}_x\text{Si}$, $\text{Fe}_{3-x}\text{Mn}_x\text{Si}$ and $\text{Mn}_2\text{V}_{1-y}\text{Al}_{1+y}$ alloys.

HA(η)	$\text{Fe}_{3-x}\text{V}_x\text{Si}$	$\text{Fe}_{3-x}\text{Mn}_x\text{Si}$	$\text{Mn}_2\text{V}_{1-y}\text{Al}_{1+y}$	
$H_{\text{hf}}(X)_0$ [kOe]	-217.8	-217.8	-66.3	
$B(X_B)$ [kOe/ μ_B]			+12.38	
$C_1(X_B)$ [kOe]	+50	+35	-29.2	
$C_1(X_B)/H_{\text{hf}}(X)_0$	-0.23	-0.16	+0.44	
$H_{\text{hf}}(Y)_0$ [kOe]	-337.7	-337.7	-85.7	
$C(Y_B)$ [kOe]	+7.5	+7.5	-9.9	
$C(Y_B)/H_{\text{hf}}(Y)_0$	-0.023	-0.023	+0.12	
$H_{\text{hf}}(\eta)_0$ [kOe]	47.7*	-258.8		
$C(\eta_B)$ [kOe]	-4.7	+5.5		
$C(\eta_B)/H_{\text{hf}}(\eta)_0$	-0.099	-0.022		
$H_{\text{hf}}(Z)_0$ [kOe]	37*	37*	-25.4	
$C(Z_B)$ [kOe]			-1.65	
$C(Z_B)/H_{\text{hf}}(Z)_0$			+0.064	
$\mu_0(X)$ [μ_B]	1.35	1.35	** 0.953	0.607
δ [μ_B]	-1.35	-1.35	0.897	1.24
$\mu_0(Y)$ [μ_B]	2.2	2.2	0	0.346
$\mu_0(\eta)$ [μ_B]	0	2.2	0	0
$\Theta(X)_{yz}$ [kOe/ μ_B]			+0.442	
$\epsilon(Y)_x$ [kOe/ μ_B] [#]			-11.24	
"	-11.11	-11.11	-22.07	-15.96
$\epsilon(\eta)_x$ [kOe/ μ_B] [#]	5.88			
"	6.96	-8.15		
$\epsilon(Z)_x$ [kOe/ μ_B] [#]	3.42	3.42	-3.33	-5.3
"			-7.36	-5.3
$H_0(X)$ [kOe/ μ_B]				
$H_1(X)_y$ [kOe/ μ_B]				
$H_0(Y)$ [kOe/ μ_B]	-98.23	-98.23	-23.60	
$H_1(Y)_x$ [kOe/ μ_B]	-11.11	-11.11	-15.96	
$H_0(\eta)$ [kOe/ μ_B]		-87.09		
$H_1(\eta)_x$ [kOe/ μ_B]		-8.15		
$K(YX)$	-0.018	-0.018		
$K(\eta X)$		-0.003		

* Absolute value, # Upper from $H_{\text{hf}}(W)_0$ and lower from $C(W_B)$

** Numerical values in the left side are calculated on the assumption of $\mu_0(Y) = 0$, and those in the right side are obtained $\mu_0(Y) \neq 0$, and by the aid of $\delta/\mu_0(X) = 32C(Z_B)/H_{\text{hf}}(Z)_0$ with nonmagnetic Z.

by Niculescu et al.⁶⁾. Fe(A,C) and Fe(B) have the moment of 1.35 and 2.2 [μ_B], respectively but V is nonmagnetic. Furthermore $\mu_0(\text{Fe})_{A,C} = -\delta$ is confirmed. In Table 4, several parameters obtained from their experiments are described together with those of $\text{Fe}_{3-x}\text{Mn}_x\text{Si}$ and $\text{Mn}_2\text{V}_{1-y}\text{Al}_{1+y}$ alloys

As the hyperfine field of the nonmagnetic elements is extensively studied only in V, the examination of $\varepsilon(\eta)_x$ described in the technique (e) is made in this case. The value of $\varepsilon(\eta)_x$ obtained from $H_{\text{hf}}(\eta)_0$ and $C(\eta_B)$ are 5.88 and 6.96, respectively with $\eta = \text{V}$, which shows the relation of $C(\eta_B)/H_{\text{hf}}(\eta)_0 = -1/s_3(\eta) = -1/12$ is also approximately realized in this case according to Eq.(33)' because of $\mu_0(X) = -\delta$, as can be seen in Table 4.

In respect of $H_{\text{hf}}(X)_0$, according to Eqs.(22) and (32) the following relation may be derived approximately on account of $\mu_0(X) = -\delta$ and $\mu_0(\eta) = 0$ in this alloy,

$$H_{\text{hf}}(X)_0 = H_0(X)\mu_0(X) + 4H_1(X)_Y\mu_0(Y)$$

$$C_1(X_B) = -(1/4)[H_0(X)\mu_0(X) + 4H_1(Y)_X\mu_0(Y)]$$

Then, putting $H_1(X)_Y = H_1(Y)_X$ because of $Y = X = \text{Fe}$ in this case, we obtain $C_1(X_B)/H_{\text{hf}}(X)_0 = -1/4$, which is comparable with the experimental result of -0.23 as described in Table 4.

Regarding $H_{\text{hf}}(Y_B)$, $H_0(Y)$ and $H_1(Y)_X$ may be obtained by the technique (c). According to Eqs.(23) and (25)', $H_0(Y) = -98.23$ and $H_1(Y)_X = -11.11$ [kOe/ μ_B] are obtained. These values are well comparable with those obtained previously in Fe_3Z alloy systems. If a small discrepancy in $H_0(Y)$ is ascribed to $K(\text{FeFe})$, it is estimated to be -0.018.

In Fig. 5, the relative intensity calculated according to Eqs. (6) and (8) is given together with the experimental results obtained by Niculescu et al.⁶⁾. As can be seen from this figure, the calculated one is in satisfactory agreement with the observed one, except those for the alloys with $x > 0.50$, as indicated by the thick vertical lines. If we imagine that some disordering occurs between the atoms in B and D sites and one third of V atoms enter the D sites, the population of V at B and D sites under the influence of V impurities are calculated, resulting the intensity indicated by the fine solid and dotted vertical lines, respectively. Therefore, some irregularity of the intensity at high V concentration may be ascribed to such a disordering of atoms between B and D atomic sites.

3. Off-stoichiometric $\text{Fe}_{3-x}\text{Mn}_x\text{Si}$ alloy

This alloy system is also investigated by Niculescu et al.⁶⁾.

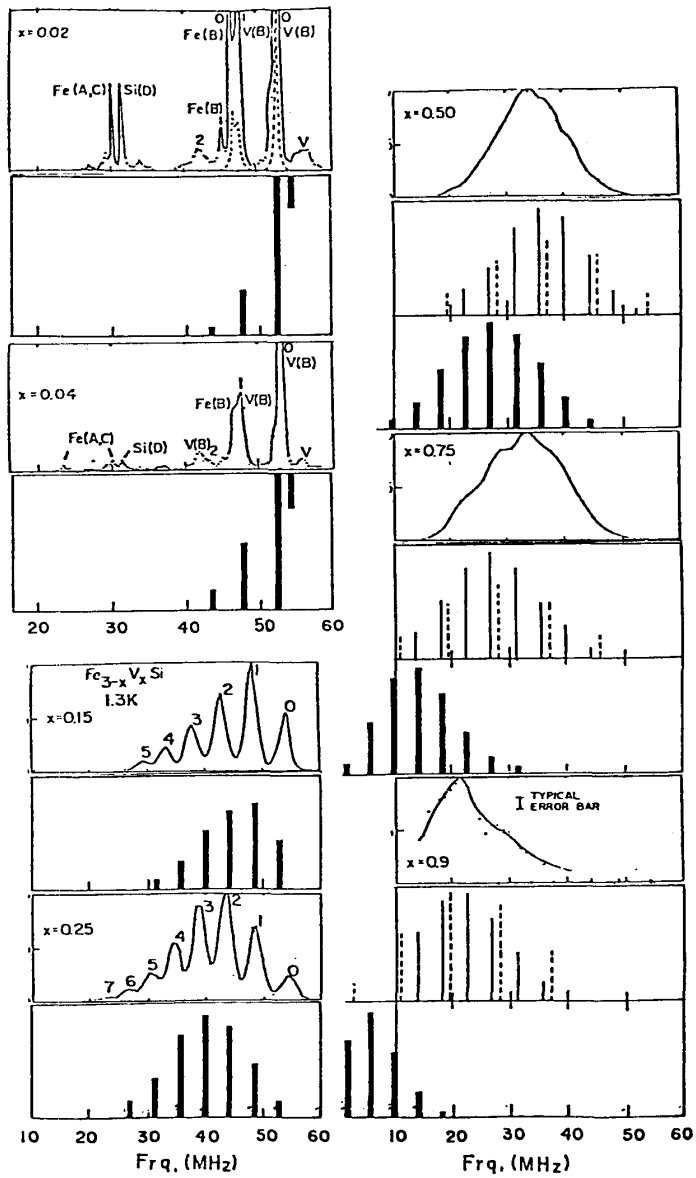


Fig. 5. NMR spin echo spectrum in $\text{Fe}_{3-x}\text{V}_x\text{Si}$ ($x = 0.02 \sim 0.90$) by Niculescu et al. (ref. to 6) and the calculated relative intensity of V according to Eq.(6). The thick vertical line corresponds to the relative intensity as all V atoms occupy the B sites. While the fine solid and dotted vertical lines correspond to the lines when V atoms occupy the B and D site in a ratio of two to one, respectively. Except the alloys with $x = 0.02$ and 0.04 , the calculated maximum population is reduced to the value of the maximum peak in the experiments.

In this case, the moment value does not change in respect of $\mu_0(X)$, δ and $\mu_0(Y)$ but change in $\mu_0(\eta)$ from 0 to 2.2 [μ_B] in comparison with the former alloy system. Therefore, it is concluded at first that the same value of $C(Y_B)$ as before is expected and in fact is realized experimentally as described in Table 4 according to Eq.(25)'.

However, $C_1(X_B)$ is varied with $H_1(\eta)_x \mu_0(\eta)$ term, which is finite because of nonvanishing $\mu_0(\eta)$ in this case. According to Eq.(32), the difference in $C_1(X_B)$ from that of $Fe_{3-x}V_xSi$ alloy system gives $H_1(Mn)_{Fe} = -8.91$ [kOe/μ_B], which has the same sign but is twice as large as the value of $H_1(Mn)_{Co}$ obtained in Co_2MnZ alloy system previously.

While $H_{hf}(\eta)_0$ and $C(\eta_B)$ with $\eta = Mn$ gives $H_0(Mn)$ and $H_1(Mn)_{Fe}$ by the aid of the technique (d). The obtained value of $H_0(Mn) = -87.63$ and $H_1(Mn)_{Fe} = -8.15$ [kOe/μ_B] are in good agreement with that obtained Co_2MnZ alloy system for the former and that obtained from $C_1(\eta_B)$ in this $Fe_{3-x}Mn_xSi$ alloy, respectively. A small discrepancy in $H_0(Mn)$ gives $K(MnFe) = -0.003$.

4. Off-stoichiometric $Mn_2V_{1-y}Al_{1+y}$ alloy

Recently in this alloy system, NMR experiments have been performed^{18),19)}. As can be seen in Fig. 6, the NMR spectrum is not so well resolved, especially in high frequency range in comparison with those of $Co_2Mn_{1.04}Si_{0.96}$ in Fig. 2 and of $Fe_{3-x}V_xSi$ in Fig. 5.

Therefore, it is somewhat difficult to assign each satellite peak. In the stoichiometric composition, three main peaks are observed at 28.2, 71.5 and 104.2 [MHz] and assigned to ^{27}Al , ^{51}V and ^{55}Mn , respectively from the behavior of each peak concerning with the relaxation time T_1 and the increasing rate of the peak position with external field¹⁸⁾. The rate for the 71 and 104 [MHz] are -1.11 ± 0.02 and -1.03 ± 0.02 [MHz/kOe]. While the expected rate is 1.1193 [MHz/kOe] for ^{51}V and 1.0553 [MHz/kOe] for ^{55}Mn ²⁰⁾. Therefore, the assignment of the peak seemed to be appropriate.

However, the satellite structures of the NMR spectrum observed at higher Al concentration shows a contradict feature with the above assignment, if the present model is also applicable to this case. The present model predicts that the number of Y satellites should be greater than X satellites. The maximum possible number is twelve for Y and four for X. The relative intensity of $W = X, Y$ varies according to Eqs.(6) and (8). Therefore, in each alloy composition one may expect that the actual peak of spectrum should correspond to the resonance peak with the maximum population in a given alloy composition. Assuming the main peak of V is situated at 71 [MHz], the resonance peak with the maximum population, which corresponds to the satellite

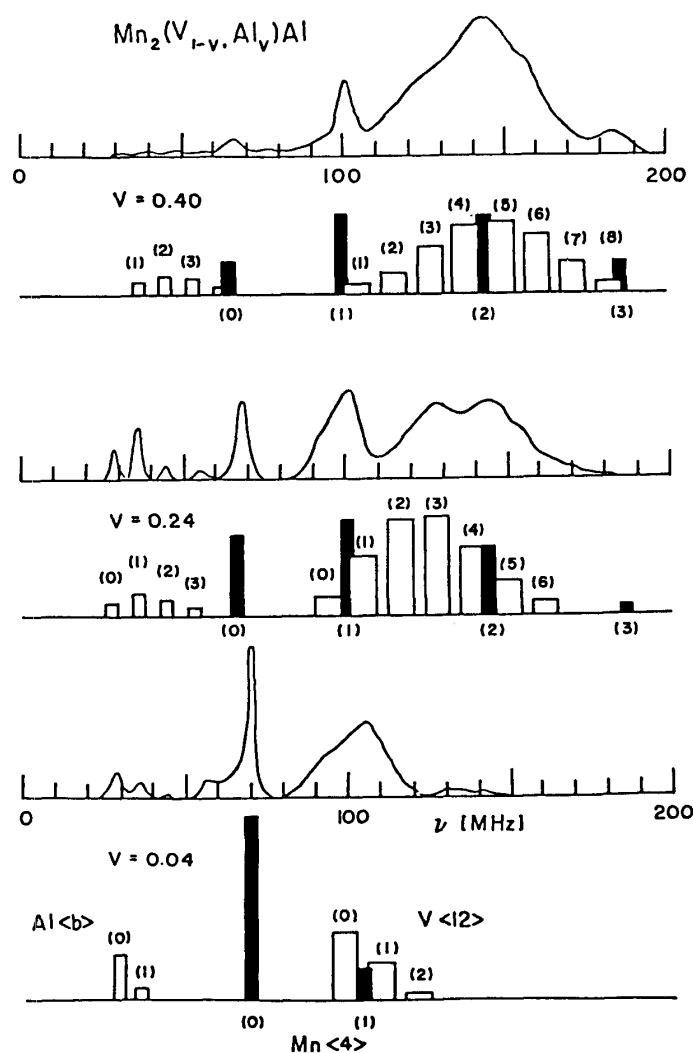


Fig. 6. NMR spin echo spectrum in $\text{Mn}_2\text{V}_{1-y}\text{Al}_y\text{Al}$ by Yoshida et al.¹⁹⁾ and its analysis described in the text. The open and closed vertical narrow bars give the relative intensity of Al and Mn, respectively. The open vertical wide bar indicate that of V.

with $n_3(\eta) = 5$ at the highest Al concentration, i. e. $v = 0.40$, must be assigned to somewhat broad peak at about 142 [MHz] in Fig. 6. Unfortunately, however, other four satellites could not be found between the main peak and the satellite peak with the maximum intensity. There is only one satellite peak. On the contrary, if the main peak of Mn is assumed to be situated at 71 [MHz], the satellite peaks with $n_1(\eta) = 1, 2$ and 3 are fairly well situated at the relatively sharp peaks

observed in the NMR spectrum at $\nu = 0.40$, as indicated by the closed vertical bar with the relative population in Fig. 6. At other alloy compositions, the correspondence between the calculated satellites of Mn and the relatively sharp peaks in experiments seems to be fairly good.

Therefore the remained peak observed at about 130 [MHz] for the alloy with $\nu = 0.24$ is used to determine the separation of the satellites of V spectrum. The parameters in Table 4 are thus obtained. In this analysis, the value of ν is a little varied from that estimated from the chemical analysis, taking into account some disordering between B and D atomic sites. Original compositions of three alloys are $\text{Mn}_{50}\text{V}_{25}\text{Al}_{25}$, $\text{Mn}_{51}\text{V}_{20}\text{Al}_{29}$ and $\text{Mn}_{51}\text{V}_{14}\text{Al}_{35}$. After such a correction the relative intensity of all the peaks are calculated according to Eqs. (6) and (8) with the weighting factor of $k(X):k(Y):k(Z) = 1:10:1$, and each peak is situated according to the parameters in Table 4. It may be recognized that the calculated one corresponds fairly well to the observed spectrum. In this analysis, the abnormally broad peak at 104 [MHz] may be understood naturally due to the superposition of the main and satellite peaks of V and furthermore the 1st satellite peak of Mn, suggesting some disordering occurs in this alloy.

Regarding the hyperfine field, we tried at first to analyze data on the assumption that Mn only is magnetic. However, either $\epsilon(Y)_x$ or $\epsilon(Z)_x$ obtained from the satellite separations is twice as large as that obtained from the main peak as described in Table 4, suggesting V atom is magnetic. Therefore, combining the results of the magnetization measurements with the value of $\delta/\mu_0(X)$ obtained from $C(Z_B)/H_{\text{hf}}(Z)_0$ according to Eq. (33), the atomic moments $\mu_0(X) = 0.607$, $\mu_0(Y) = 0.346$ and $\delta = 1.24$ [μ_B] are obtained on the assumption of a simple ferri- or ferromagnetic structure in this alloy.

Utilizing these values and $H_0(\text{Mn}) = -86.57$ [kOe/μ_B] obtained previously, one may calculate $H_{\text{hf}}(\text{Mn})_0 = -59.00$ [kOe], if $H_1(\text{Mn})_{\text{Co}} = -4.66$ [kOe/μ_B] is used instead of real $H_1(\text{Mn})_V$ or $H_0(\text{Mn}) = -63.82$ [kOe], if $H_1(\text{Mn})_{\text{Fe}} = -8.15$ [kOe/μ_B] is used. While experimentally $H_{\text{hf}}(\text{Mn})_0 = -66.3$ [kOe] as described in Table 4. Since in this case V is magnetic $H_0(V) = -23.60$ [kOe/μ_B] and $H_1(V)_{\text{Mn}} = -15.96$ [kOe/μ_B] are obtained in a similar way as made in $\text{Fe}_{3-x}\text{V}_x\text{Si}$ alloy for Fe(B). However, an obtained $\mu_0(V)$ is rather suspicious and therefore the conclusive analysis must be postponed until the direct determination of the magnetic structure is made on this alloy by the neutron diffraction measurements.

VII. Conclusion

Developing the idea of Niculescu et al.⁶⁾, we obtained the phenomenological expression of the hyperfine field of a nucleus as functions of the moments of the constituent elements in Heusler alloys. Even in an alloy such as $X_2(Y_{1-y}Z_y)$ containing the impurity η , the moments in the expression are only limited to those in the stoichiometric alloy X_2YZ as well as the increment of the moment of X , which are able to be determined by neutron diffraction measurements directly. This fact is helpful to the analysis of the NMR experiments.

The hyperfine field of a nucleus in an alloy containing impurities consists of three parts, namely the constant term, the composition dependent term and the discrete term dependent upon the number of the neighbouring impurities around the nucleus. In the NMR spectrum, the first term corresponds to the main peak of the nucleus, which expresses the hyperfine field of the nucleus of the stoichiometric alloy, the second one gives the shift of each resonance peak with alloy composition and the third one causes the occurrence of the satellite peaks and gives their separation.

Several ratios of the field to moment are also given and applied successfully to the analysis of the NMR experiments. By the aid of these ratios, two sets of the hyperfine field coefficients are obtained in Co_2MnZ and Fe_3Z alloy systems and their usefulness is verified in the determination of the hyperfine field of a nucleus in another atomic site. The hyperfine field coefficients are also determined in two alloy systems $Fe_{3-x}V_xSi$ and $Fe_{3-x}Mn_xSi$ independently by use of the information of the satellite separation and give values, which are in good agreement with those obtained from Co_2MnZ and Fe_3Z . Furthermore, the predicted relation between the ratio of the satellite separation to the hyperfine field of the main peak and the ratio of the moment variation rate to the moment of X atom of the stoichiometric alloy for the nonmagnetic element in general and for X element in special, is confirmed satisfactorily. This relation is also applied to $Mn_2V_{1-y}Al_{1+y}$ alloy system and suggests strongly that V atom is also magnetic in addition to Mn in this alloy system.

The relative intensity of the main and satellite peaks of a nucleus is calculated on the assumption that the intensity of each resonance peak is proportional to the population of the resonating nucleus characterized by its special local environment, which determines the position of each resonance peak. The calculated relative intensity is in fairly good agreement with the NMR spectrum in $Fe_{3-x}V_xSi$ alloy system and is useful to the analysis of a rather complex spectrum in $Mn_2V_{1-y}Al_{1+y}$ alloy system.

Since the fundamental equations used to develop the hyperfine field expressions are applicable to any magnetic alloy with the structure other than $L2_1$ structure, one may expect that the validity of the present model will be examined also in other magnetic alloy systems as made in the present work in Heusler alloys.

Acknowledgements

The author wishes to express his sincere thanks to Dr. H. Itoh, Mr. Y. Yoshida and Mr. M. Hirai in the cooperation of the experimental study of magnetism in Heusler alloys. He is also much indebted to Prof. W. Kawakami of Kagoshima University in NMR experiments. This work was supported by the Grant-in-aid of Fundamental Scientific Research from the Ministry of Education.

References

- (1) A.J. Bradley and J.W. Rogers, Proc. Roy. Soc., A144 (1934), 340.
- (2) F. Heusler, Verhandl. deu. physik. Ges., 5 (1903), 219.
- (3) W.B. Pearson, Handbook of Lattice Spacings and Structures of Metals and Alloys, (Pergamon Press, New York, 1958), pp. 120.
- (4) T. Ohoyama and K. Endo, Magnetic Properties of Heusler Alloys and the Related Intermetallic Compounds, Report of the Physical and Chemical Property Data, Magnetic Property Data, Vol. 4, ed. by S. Iida (Promotion Bureau Science & technology Agency, 1979), pp. 73
- (5) M. Hirai, Master Thesis of Tohoku Univ. (1981)
- (6) V. Niculescu, K. Raj, J.I. Budnick, J.T. Burch, W.A. Heines and A.H. Menotti, Phys. Rev., 14 (1976), 4160; V. Niculescu, T.J. Burch, K. Raj and J.I. Budnick, J. Mag. Mag. Materials, 5 (1977), 60.
- (7) J.C. Suits, Solid State Commun., 18 (1976), 425.
- (8) S. Tomiyoshi and H. Watanabe, J. Phys. Soc. Japan, 39 (1975), 295
- (9) A.K. Grover, Le Dang Khoi and P. Veillet, J. Phys. F (Metal Phys.) 8 (1978), 1557.
- (10) Y. Nakamura and M. Mekata, Ordered Alloys, Handbook of Magnetic Matter, ed. by S. Chikazumi et al. (Asakura Book Comp. 1975), pp. 356.
- (11) N.K. Jaggi, K.R.P.M. Rao, A.K. Grover, L.C. Gupta, R. Vijayaraghavan and Le Dang Khoi, Hyperfine Interactions, 4 (1978), 402
- (12) Le Dang Khoi, P. Veillet and I.A. Campbell, Physica, 86-88B (1977), 413.

- (13) P.A. Beck, *Metall. Trans.*, 2 (1971), 2015.
- (14) B. Caloli and A. Blandin, *J. Phys. Chem. Solids*, 27 (1966), 503.
- (15) P.J. Webster, *J. Phys. Chem. Solids*, 32 (1971), 1221.
- (16) T. Shinohara, *J. Phys. Soc. Japan* 28 (1970), 313.
- (17) Le Dang Khoi, P. Weillet and I.A. Campbell, *J. Phys. F (Metal Phys.)* 18 (1978), 1811.
- (18) M. Kawakami, Y. Yoshida, T. Nakamichi, S. Ishida and H. Enokiya, *J. Phys. Soc. Japan*, 50 (1981), 1041.
- (19) Y. Yoshida, M. Kawakami and T. Nakamichi, *J. Phys. Soc. Japan*, to be submitted; Y. Yoshida, Master Thesis of Tohoku Univ. (1980)
- (20) G.E. Pake, *Solid State Physics*, ed. Seitz and Turnbull, (Academic Press, New York, 1956), Vol. 2, pp. 3